Title: Anti-EDAR Agonist Antibody Therapy Resolves Palate Defects in *Pax9*$^{-/-}$ Mice

Authors: Jia S., Zhou J., Wee Y., Mikkola M.L., Schneider P., D'Souza R.N.,

Journal: Journal of Dental Research,

Year: 2017

Volume: 96(11)

Pages: 1282-1289

DOI: 10.1177/0022034517726073

Anti-EDAR Agonist Antibody Therapy Resolves Palate Defects in *Pax9*$^{-/-}$ Mice

Shihai Jia[1], Jing Zhou[1], Yinshen Wee[1], Marja L. Mikkola[2], Pascal Schneider[3], Rena N. D'Souza[1,4,*]

[1]School of Dentistry and [4]Departments of Neurobiology & Anatomy, Pathology, School of Medicine, University of Utah, Salt Lake City, Utah 84112, USA.

[2]Developmental Biology Program, Institute of Biotechnology, University of Helsinki, 00014 Helsinki, Finland.

[3]Department of Biochemistry, University of Lausanne, CH-1066 Epalinges, Switzerland.

*__Corresponding author__:

Rena D'Souza, DDS, MS, PhD

Professor

School of Dentistry and Departments of Neurobiology & Anatomy, Pathology, School of Medicine, University of Utah

75 South 2000 East

Salt Lake City, UT 84112

USA

Phone: (801) 587-1203; Fax: (801) 581-8964

Email: rena.dsouza@hsc.utah.edu

Abstract

To date, surgical interventions are the only means by which craniofacial anomalies can be corrected so that function, esthetics, and the sense of well-being are restored in affected individuals. Unfortunately, for patients with cleft palate—one of the most common of congenital birth defects—treatment following surgery is prolonged over a lifetime and often involves multidisciplinary regimens. Hence, there is a need to understand the molecular pathways that control palatogenesis and to translate such information for the development of noninvasive therapies that can either prevent or correct cleft palates in humans. Here, we use the well characterized model of the Pax9−/− mouse, which displays a consistent phenotype of a secondary cleft palate, to test a novel therapeutic. Specifically, we demonstrate that the controlled intravenous delivery of a novel mouse monoclonal antibody replacement therapy, which acts as an agonist for the ectodysplasin (Eda) pathway, can resolve cleft palate defects in Pax9−/− embryos in utero. Such pharmacological interventions did not reverse the arrest in tooth, thymus, and parathyroid gland development, suggesting that the relationship of Pax9 to the Eda/Edar pathway is both unique and essential for palatogenesis. Expression analyses and unbiased gene expression profiling studies offer a molecular explanation for the resolution of palatal defects, showing that Eda and Edar-related genes are expressed in normal palatal tissues and that the Eda/Edar signaling pathway is downstream of Pax9 in palatogenesis. Taken together, our data uncover a unique relationship between Pax9 and the Eda/Edar signaling pathway that can be further exploited for the development of noninvasive, safe, and effective therapies for the treatment of cleft palate conditions and other single-gene disorders affecting the craniofacial complex.

Keywords: Developmental biology, Cleft palate, craniofacial biology/genetics, morphogenesis, gene expression, therapeutic treatment.

Introduction

Disruptions in craniofacial development lead to a spectrum of malformations that comprise over one-third of all congenital birth defects and often lead to devastating clinical and psychosocial consequences. Most of these disorders involve mineralizing tissues, such as the cranial and facial sutures, the palate and tooth organs, as well as the maxilla and mandible (Szabo- Rogers et al. 2010; Twigg and Wilkie 2015). Despite the advances made in our understanding of the genetic etiology and mechanisms responsible for these conditions, treatment options are restricted to surgical interventions that, if successful, require life-long care. Hence, there is a critical need to develop novel therapies that are biologically driven, minimally invasive, safe, and effective.

Classified as the most common among craniofacial disorders are clefts of the palate and lip, which occur in 1 per 700 live births worldwide and present with a heterogenous etiology involving both genetic and environmental risk factors (Mossey et al. 2009; Dixon et al. 2011; Leslie and Marazita 2013; Beaty et al. 2016). Significant progress has been made in unraveling the causes of syndromic and nonsyndromic (isolated) forms of cleft palate using a combination of analytical approaches: whole genome sequencing, whole-exome sequencing, genome-wide association analyses, and carefully executed epidemiologic and phenotypic characterization studies (Beaty et al. 2016; Leslie and Marazita 2013). Furthermore, studies of genetically engineered mice with cleft palate phenotypes have underscored the importance of the transforming growth factor (TGF)-β, fibroblast growth factor (FGF), WNT, hedgehog, and mitogen activated protein kinase (MAPK) signaling pathways in palatogenesis (Funato et al. 2015). Among the 180 mouse cleft genes identified through gene ontology analyses, transcription factors, particularly those with homeobox-containing domains, are the most significantly enriched in palatogenesis (Funato et al. 2015). This improved understanding of the mechanisms that drive normal and abnormal palatogenesis and the array of diagnostic tools

readily available provide opportunities to prevent or reverse palatal defects in a manner that will reduce morbidity and mortality, obviate the need for surgery, and reduce patient dependence on life-long multidisciplinary care.

Pax9 is known to play a key role in palatogenesis and in the development of tooth organs and other pharyngeal pouch derivatives. Its deficiency consistently leads to cleft of the secondary palate, along with arrests in tooth, thymus, and parathyroid gland development (Peters et al. 1998). Studies by Zhou et al. (2013) point to a role for Pax9 in the patterning of the anterior-posterior (AP) axis and palatal shelf outgrowth through its control of cell proliferation and its interactions with the Bmp, Fgf, and Shh pathways (Zhou et al. 2013).

However, there is much to learn about the relationship between Pax9 and other signaling pathways during palatogenesis. Our recent studies have shown that Pax9 shares an upstream molecular relationship with Wnt pathway genes during palate formation (unpublished data). Wnt genes encode a family of secreted signaling proteins that regulate developmental processes critical for palatogenesis, such as early patterning, cell proliferation, differentiation, and apoptosis. Several reports confirm that Wnt signaling is linked with the ectodysplasin/ ectodysplasin A receptor (Eda/Edar) pathway during hair follicle, tooth, and mammary gland development (Laurikkala et al. 2001; Zhang et al. 2009; Voutilainen et al. 2015). Since Pax9 is involved with Wnt signaling during palatogenesis, the focus of this study was to evaluate whether the Eda/Edar signaling pathway is involved with Pax9 during palate formation and whether such a relationship could be exploited for pharmacological interventions aimed at correcting palatal defects in Pax9−/− mice.

Our approaches have been inspired by the successes of using recombinant EDA (rEDA) protein for the treatment of X-linked hypohidrotic ectodermal dysplasia (XL-HED), a syndrome caused by mutations in the EDA gene, which encodes a ligand in the tumor necrosis factor (TNF)/EDA signaling pathway. XL-HED is characterized by a failure of hair, tooth, and

gland development (Monreal et al. 1998). A few timely injections of rEDA protein can correct all XL-HED defects in Eda-deficient Tabby mice permanently (Gaide and Schneider 2003). Both rEDA protein and an agonist EDA-receptor monoclonal antibody (mAbEDAR) are capable of permanently correcting the dental phenotypes of XL-HED in mice and especially dogs, with the rescue of permanent dentition following EDA treatment in early postnatal life (Casal et al. 1997; Kowalczyk et al. 2011; Mauldin et al. 2009).

The results of our expression and molecular analyses demonstrate for the first time that Pax9 shares an upstream molecular relationship with the Eda/Edar signaling pathway during in vivo palatogenesis. The importance of these interactions is underscored by our findings that an agonist anti-EDAR monoclonal antibody, when administered in utero, reverted secondary palate clefts in Pax9−/− mouse embryos. Taken together, these data advance our knowledge about palatogenesis and help to explain the mechanism underlying the resolution of the cleft defects in Pax9−/− mice.

Materials and methods

Mouse Strains and Tissues

All animal procedures were approved by the Institutional Animal Care and Use Committee (IACUC) at the University of Utah (Protocol #17-02004). Breeding pairs of Pax9+/− mice were provided by Dr. Rulang Jiang (Cincinnati Children's Hospital; Zhou et al. 2011) and maintained on a C57BL/6 background with 2- to 8-month-old females for intercross mating. Whole heads were obtained from NF-κB-LacZ reporter mice staged from E12.5 to E15.5 and staining for beta-galactosidase activity was performed as described by Bhakar et al. (2002).

Expression and Activity Studies

In situ hybridizations were performed using digoxigenin-labeled RNA probes to Eda, Edar and Col1a1, as described previously (D'Souza et al. 1993; Zhang et al. 1999; Zhou et al. 2013). For whole-mount in situ hybridization, a 2 μg/ml antisense RNA probe was loaded onto each

sample, and an antidigoxigenin-AP antibody (11093274910, Roche, 1:2,000) was used to detect the labeled probe. For section in situ hybridization, a 1 μg/ml antisense RNA probe was loaded onto each position-matched section and anti-digoxigenin-AP antibody (1:1,000) was used to detect the labeled probe. Comparable images were taken by digital microscope (EVOS). At least 5 replicates were performed for each assay. For whole-mount X-gal staining of Eda/Edar signaling activity, the whole heads of NF-κB reporter embryos from E12.5 to E15 were fixed in 4% paraformaldehyde after removal of the lower jaw, then treated as previously described (Voutilainen et al. 2015).

Delivery of mAbEDAR monoclonal antibody and histological analysis

The anti-EDAR monoclonal antibody 1 (hereafter referred to as mAbEDAR) was injected into the tail vein of timed pregnant females, as previously described (Kowalczyk et al. 2011). The dosage of 16 mg/kg of body weight was calculated based on a

half-life (t 1/2) of the antibody estimated to be 10 days. Hence, a single injection at E10.5—one day preceding the initiation of palatogenesis—was sufficient to cover critical events that occur from E11.5 to E15.5 of embryogenesis. A second injection at E12.5 was delivered to study the effects of an extra burst of signaling activity at a time of palatal shelf outgrowth. The same amount of bovine serum albumin diluted in phosphate-buffered saline was delivered to the controls. Embryos were fixed in 4% paraformaldehyde overnight and serial coronal sections were stained with hematoxylin and eosin for morphologic evaluation. Position-matched sections were stained with Masson's trichrome to evaluate connective tissue deposition (Chen et al. 2009).

RNAseq and Real-Time RT-PCR analyses

Whole-transcriptome profiling of the developing palatal shelves was performed by RNA-Seq and data were collated at the High-Throughput Genomics and Bioinformatics Analysis Core Facility (University of Utah). In brief, after total RNAs were extracted from individual samples, cDNA libraries were generated using the Illumina TruSeq RNA Sample Prep Kit v2 with oligo(dT)

selection (Jia et al. 2013). Read counts were generated using USeq's Defined Region Differential Seq application and normalized counts were used in DESeq2 to measure differential expression. The RNA-seq raw data have been deposited into Gene Expression Omnibus database (GEO) (http://www.ncbi.nlm.nih.gov/geo) under the accession number, GSE89603. For real-time RT-PCR, first-strand cDNA was synthesized using the SuperScript First-Strand Synthesis System (Thermo Fisher Scientific). Quantitative PCRs were performed in a StepOnePlus Real Time RT-PCR System (Applied Biosystems) using the SYBR Green qPCR Supermix (Thermo Fisher Scientific). The list of primer sets is provided in Appendix Table 1. Five sets of samples were analyzed for each gene, and a Student's **t**-test was used to analyze differences, with **P** values of <0.01 considered statistically significant.

Results

Pax9 shares a molecular relationship with the Eda/Edar signaling pathway during palatogenesis

Since the expression of Eda/Edar pathway genes has not been studied in normal and Pax9−/−palatal shelves, we first examined the differential expression of Eda/Edar genes in these tissues. Comparing the unbiased set of RNAseq data obtained from dissected Pax9+/+ and Pax9−/− E13.5 palatal shelves, we determined normalized raw counts for each of the Eda/Edar signaling pathway-related genes. As shown in Fig. 1A, the expression of Edar was significantly reduced in Pax9−/−samples ($P < 0.01$). The 2-fold reduced expression level of Edar in Pax9−/−palate was confirmed by real-time RT-PCR (Fig. 1B).

To better assess the function of the Eda/Edar signaling pathway in palatogenesis, we analyzed Eda/Edar signaling activity during palate formation using NF-κB reporter mice. The transcription factor, NF-κB, is a downstream mediator of Eda/Edar signaling. As Appendix Fig. 1 shows, NF-κB activity in the palate was lost in Eda−/− background, confirming that the reporter expression is a reliable indicator of Eda/Edar signaling activity during palatogenesis. We

analyzed Eda/Edar signaling activity using NF-κB reporter embryos staged from E12.5 to E15 (Fig. 2A–D). X-gal wholemount staining showed that, at E12.5, the domain of NF-κB activity started to appear at the center of the lingual edge (Fig. 2A) and extended along the edge of palate at E13 (Fig. 2B). At E14, the activities appeared throughout the lingual edge of the palate and on the palatal rugae (Fig. 2C). After palate fusion at E15, lac Z staining was only retained on the rugae (Fig. 2D). These results indicate that Eda/Edar signaling is active during palatogenesis, and that the activity is affected in Pax9−/−samples.

Compared with NF-kB activity, whole-mount in situ hybridization showed that endogenous Edar mRNA transcripts had a broader expression, with higher expression seen in the lingual region and lower expression in the buccal region of the developing Pax9+/− palate shelves (Fig. 2E, I). The lingual expression domain for Edar transcripts appeared to be reduced in Pax9−/− palatal shelves (Fig. 2F, J). Interestingly, Eda showed a lingual–buccal gradient of expression at E13.5, with the domain of expression becoming restricted to the lingual region of the posterior palatal shelves at E14.5 (Fig. 2G, K). In Pax9−/−palates, Eda expression resembled that seen in Pax9+/− shelves at E13.5 but was far more diffuse at E14.5 (Fig. 2H, L).

Treatments using mAbEDAR reverse cleft palate defects in *Pax9*$^{-/-}$ mice.

The agonist monoclonal antibody mAbEDAR, when administered in a timely manner to mice and dogs, serves as an effective pharmacological intervention for XLHED (Kowalczyk et al. 2011). Here, we delivered 16 mg/kg/body weight of mAbEDAR to Pax9−/− embryos through tail vein injection of timed pregnant Pax9+/−female mice (Fig. 3A). A single injection administered at E10.5 resulted in a 71.4% success rate of secondary palate closure (10/14 Pax9−/− embryos) (Fig. 3B). The second delivery schedule, comprising 2 separate injections at E10.5 and E12.5, resulted in 90% closure of secondary palate defects (9/10 Pax9−/−embryos) (Fig. 3B). Stereoscope evaluation of palates from mAbEDAR-treated samples showed that palatal shelf fusion had occurred in the midline after mAbEDAR treatments (Fig. 4C). Whereas mAbEDAR

therapy resulted in closure of the secondary palate, the morphology of the rugae did not appear to be fully restored (Fig. 4C). In comparison, Pax9+/+ embryos from control litters that did not receive mAbEDAR showed closed palates with parallel morphology of rugae (Fig. 4A). Pax9−/−embryos from control treatment litters showed complete cleft secondary palates, as shown in Fig. 4B.

We observed residual defects in 4 of 10 Pax9−/− embryos derived from litters that received a single injection of mAbEDAR and in 3 of 9 mutant embryos from litters treated with 2 injections of mAbEDAR. As shown in Appendix Fig. 2C, these residual defects were clearly visible in fusion zones between primary and secondary palates. Histological evaluation of position-matched, hematoxylin- and eosin-stained coronal sections of E18.5 embryos, showed normal palate fusion in wildtype controls (Fig. 4D) whereas the palate clefts of Pax9−/− controls showed no correction (Fig. 4E). Pax9−/− palate shelves exposed to mAbEDAR were fused in the midline region (Fig. 4F). The correction of secondary palate clefts in Pax9−/− mice did not prolong their survival after birth and the arrests in tooth, thymus, parathyroid glands, and hind limb development were not reversed after mAbEDAR treatment. Importantly, histopathologic and MRI analyses of Pax9+/− mothers and siblings exposed to mAbEDAR showed no long-term adverse effects on major organ systems (data not shown).

Therapeutic treatments with mAbEDAR result in osteogenesis of the palatal shelves.

We next confirmed that the effects of mAbEDAR therapy culminate in palatal osteogenesis and subsequent fusion, and was not limited to soft tissue apposition alone, as has been reported for submucosal cleft palates, a clinical phenotype described in the literature (Weatherley-White et al. 1972; Garcia Velasco et al. 1988;). We compared Masson's trichrome staining patterns with that of type I collagen (Col1a1) mRNA expression in experimental and control groups. Masson's trichrome observed in mAbEDAR-treated Pax9−/− tissues closely resembled that in Pax9+/− tissues, and indicated newly deposited connective tissue (blue color)

in both the anterior and posterior zones of the palate (Fig. 5 A–F). Positive expression of Col1a1, a marker of differentiated osteoblasts, is indicative of active osteogenic zones within palatal shelves in treated Pax9+/− embryos (Fig. 5G, J). In contrast, untreated Pax9−/− samples failed to show Col1a1 expression within the stunted palatal shelf mesenchyme (Fig. 5H, K). After mAbEDAR monoclonal antibody treatment, true fusion of the secondary palate was evident, as shown by Col1a1 expression in osteoblasts present within the anterior and posterior zones of the palatal shelves (Fig. 5I, L).

Discussion

Our studies demonstrate for the first time that the Eda/Edar signaling pathway of genes mediate the function of Pax9 in murine palatogenesis. Of significance, is the fidelity with which the controlled intravenous delivery of mAbEDAR—a mouse agonist anti-EDAR monoclonal antibody—can activate endogenous EDAR. Data from our unbiased studies of gene expression profiles in whole Pax9−/− palatal shelves using RNA-Seq and real-time PCR analyses showed that Pax9 deficiency leads to a 2-fold down-regulation of Edar, the only receptor that binds Eda1 (the longest and only isoform of Eda critically involved in morphogenesis). Thus, the corrective actions of mAbEDAR can be explained by its ability to counteract the effect of reduced EDAR expression caused by the absence of Pax9. This conclusion is supported by the findings that the size of the sebaceous glands and the amount of sebum secretion in Eda-deficient animals exceeds that of the wildtype littermates receiving identical doses of mABEDAR1 (Kowalczyk-Quintas et al. 2015). Hence, EDAR activity in Pax9−/− mice treated with mAbEDAR can restore Eda signaling to functional levels and result in closure of the palatal shelves, as shown by the outgrowth of the palatal shelves and bone deposition toward the midline. These findings provide compelling in vivo evidence that Pax9 shares an upstream relationship with the Eda/Edar signaling pathway.

Our expression analyses reveal that NF-κB reporter gene expression in the forming palate is temporally and spatially regulated. Edar mRNA transcripts appear restricted to the lingual domain of the palatal shelves, and are less abundant in the developing palate. Interestingly, Eda mRNA transcripts appear more spatially diffuse in the palatal shelves; although, the levels of expression were not drastically altered in the absence of Pax9. Taken together, these studies describe a unique relationship between Pax9 and the Eda/Edar signaling pathway in palatogenesis while offering a new approach for the treatment of cleft palate defects in utero.

Pax9 is important for the patterning of the AP axis during murine palatogenesis and its interactions with the Bmp, Fgf and Shh pathways stimulate cell proliferation and the subsequent of the palatal shelves (Peters et al. 1998; Zhou et al. 2013). More recently, our research group has shown that the Wnt genes are key mediators of Pax9 function in the posterior domain of palatal mesenchyme (unpublished data). During the formation of ectodermal appendages, like hair follicles and tooth organs, there is a strong interdependence between Wnt and Eda/Edar signaling pathways (Laurikkala et al. 2001; Zhang et al. 2009). Such a complex interplay between these 2 pathways is also evident in mammary gland bud development, where Wnt genes are transcriptional targets of Eda/Edar signaling (Voutilainen et al. 2015).

Hence, Eda/Edar signaling is also needed for the development of organs other than ectodermal appendages, suggesting a broader role for this pathway in organogenesis. Since the Eda/Edar system is an important effector of canonical Wnt signaling in developing skin appendages, future studies must delineate whether Pax9 shares a direct molecular relationship with the Eda/Edar signaling pathway during palatogenesis or whether its actions are mediated via Wnt genes.

Our studies show that agonist anti-EDAR antibodies can correct cleft defects in Pax9−/−embryos. However, downless mice harboring a spontaneous missense mutation in Edar had defective ectodermal organs and disordered patterns of rugae without cleft palate

defects (Headon and Overbeek 1999; Laurikkala et al. 2002). Clefts of the secondary palate are also not observed in Edadeficient dogs (Casal et al. 1997) and mutations in EDA genes have not yet been associated with cleft palate/lip defects in humans. If the overstimulation of Edar with agonists would compensate for the loss of one or several other Pax9 targets, for example Wnts, which have been shown to act both upstream and downstream of Edar (Zhang et al. 2009; Laurikkala et al. 2001), this could explain why Eda/Edar signaling is dispensable for palate formation yet able to substitute for the functions of Pax9 in palatogenesis.

The availability of pharmacological activators of the Eda/ Edar pathway has advanced treatment strategies for the correction of specific XLHED symptoms in humans (Dr. Holm Schneider, personal communications). As reviewed by Kowalczyk-Quintas and Schneider (2014), Eda-deficiency in animal models can be corrected by the controlled delivery of soluble EDAR agonists that precisely target affected ectodermal appendages and lead to the permanent correction of adverse phenotypes affecting hair, sweat glands, and tooth organs. Because of their long half-life after injection in vivo, agonist anti-EDAR mouse monoclonal antibodies are safe and effective in mice, with no signs of neutralizing immune response (Kowalczyk et al. 2011), even after chronic administration for months (Kowalczyk-Quintas et al. 2015). Furthermore, expression levels of Bmp4, Msx1, and Osr2, which are significantly downregulated in the absence of Pax9, are not restored after treatment with mAbEDAR (Appendix Fig. 3 and 4). This suggests that the signaling hierarchy involving Pax9 and the Eda/Edar pathway, while critical for a palate formation, may not involve these molecules. In these studies, it is intriguing that mAbEDAR therapy failed to correct other Pax9−/− defects, such as arrests in tooth, thymus, and parathyroid gland development (data not shown). Correction of other organ defects caused by Pax9 deficiency may therefore require a different dosage and/or delivery schedules of mAbEDAR.

In summary, our studies offer fresh molecular insight into the relationship between Pax9 and the Eda/Edar signaling pathway during murine palatogenesis. The use of an antibody

agonist therapy that targets the Eda/Edar pathway to specifically reverse secondary palate clefts in Pax9−/−mice offers promise for future translational studies. Such an approach and other strategies can test the use of pharmacologic modulators of key signaling pathways for the treatment of other human single-gene disorders of the craniofacial complex.

Acknowledgments:

We thank Dr. Irma Thesleff for valuable feedback on the role of the Eda/Edar pathway in palatogenesis. The technical assistance of Mr. Greg Pratt is also acknowledged.

Author Contributions

S. Jia, contributed to design, data acquisition, analysis, and interpretation, drafted and critically revised the manuscript; J. Zhou, contributed to design, data acquisition, analysis, and interpretation, critically revised the manuscript; Y. Wee, contributed to data acquisition and analysis, critically revised the manuscript; M.L. Mikkola, P. Schneider, contributed to data acquisition, critically revised the manuscript; R.N. D'Souza, contributed to conception, design, data analysis, and interpretation, drafted and critically revised the manuscript. All authors gave final approval and agree to be accountable for all aspects of the work.

Funding

The following grants from the National Institutes of Health have supported this research: DE019471, DE019471, DE019471-ARRA supplement to R.D.S; P.S. is supported by grants from the Swiss National Science Foundation and by project funding from Edimer Pharmaceuticals. M.L.M was supported by grants from the Academy of Finland and Sigrid Jusélius Foundation.

Competing Interests

P.S. is shareholder of Edimer Pharmaceuticals. Other authors declare no competing financial interests.

Data availability:

The RNA-seq raw data have been deposited into NCBI Gene Expression Omnibus database (GEO) (http://www.ncbi.nlm.nih.gov/geo) under accession number GSE89603. All material requests and correspondence should be addressed to R.D.S. (rena.dsouza@hsc.utah.edu)

References

Beaty TH, Marazita ML, Leslie EJ. 2016. Genetic factors influencing risk to orofacial clefts: Today's challenges and tomorrow's opportunities. F1000Res. 5:2800.

Bhakar AL, Tannis LL, Zeindler C, Russo MP, Jobin C, Park DS, MacPherson S, Barker PA. 2002. Constitutive nuclear factor-kappa b activity is required for central neuron survival. J Neurosci. 22(19):8466-8475.

Casal ML, Jezyk PF, Greek JM, Goldschmidt MH, Patterson DF. 1997. X-linked ectodermal dysplasia in the dog. J Hered. 88(6):513-517.

Chen J, Lan Y, Baek JA, Gao Y, Jiang R. 2009. Wnt/beta-catenin signaling plays an essential role in activation of odontogenic mesenchyme during early tooth development. Dev Biol. 334(1):174-185.

D'Souza RN, Niederreither K, de Crombrugghe B. 1993. Osteoblast-specific expression of the alpha 2(i) collagen promoter in transgenic mice: Correlation with the distribution of tgf-beta 1. J Bone Miner Res. 8(9):1127-1136.

Dixon MJ, Marazita ML, Beaty TH, Murray JC. 2011. Cleft lip and palate: Understanding genetic and environmental influences. Nat Rev Genet. 12(3):167-178.

Funato N, Nakamura M, Yanagisawa H. 2015. Molecular basis of cleft palates in mice. World J Biol Chem. 6(3):121-138.

Gaide O, Schneider P. 2003. Permanent correction of an inherited ectodermal dysplasia with recombinant eda. Nat Med. 9(5):614-618.

Garcia Velasco M, Ysunza A, Hernandez X, Marquez C. 1988. Diagnosis and treatment of submucous cleft palate: A review of 108 cases. Cleft Palate J. 25(2):171-173.

Headon DJ, Overbeek PA. 1999. Involvement of a novel tnf receptor homologue in hair follicle induction. Nature genetics. 22(4):370-374.

Jia S, Zhou J, Gao Y, Baek JA, Martin JF, Lan Y, Jiang R. 2013. Roles of bmp4 during tooth morphogenesis and sequential tooth formation. Development. 140(2):423-432.

Kowalczyk-Quintas C, Schneider P. 2014. Ectodysplasin a (eda) - eda receptor signalling and its pharmacological modulation. Cytokine Growth Factor Rev. 25(2):195-203.

Kowalczyk-Quintas C, Schuepbach-Mallepell S, Willen L, Smith TK, Huttner K, Kirby N, Headon DJ, Schneider P. 2015. Pharmacological stimulation of edar signaling in the adult enhances sebaceous gland size and function. J Invest Dermatol. 135(2):359–368.

Kowalczyk C, Dunkel N, Willen L, Casal ML, Mauldin EA, Gaide O, Tardivel A, Badic G, Etter AL, Favre M et al. 2011. Molecular and therapeutic characterization of anti-ectodysplasin a receptor (edar) agonist monoclonal antibodies. The Journal of biological chemistry. 286(35):30769-30779.

Laurikkala J, Mikkola M, Mustonen T, Aberg T, Koppinen P, Pispa J, Nieminen P, Galceran J, Grosschedl R, Thesleff I. 2001. Tnf signaling via the ligand-receptor pair ectodysplasin and edar controls the function of epithelial signaling centers and is regulated by wnt and activin during tooth organogenesis. Dev Biol. 229(2):443-455.

Laurikkala J, Pispa J, Jung HS, Nieminen P, Mikkola M, Wang X, Saarialho-Kere U, Galceran J, Grosschedl R, Thesleff I. 2002. Regulation of hair follicle development by the tnf signal ectodysplasin and its receptor edar. Development. 129(10):2541-2553.

Leslie EJ, Marazita ML. 2013. Genetics of cleft lip and cleft palate. Am J Med Genet C Semin Med Genet. 163C(4):246-258.

Mauldin EA, Gaide O, Schneider P, Casal ML. 2009. Neonatal treatment with recombinant ectodysplasin prevents respiratory disease in dogs with x-linked ectodermal dysplasia. American journal of medical genetics Part A. 149A(9):2045-2049.

Monreal AW, Zonana J, Ferguson B. 1998. Identification of a new splice form of the eda1 gene permits detection of nearly all x-linked hypohidrotic ectodermal dysplasia mutations. Am J Hum Genet. 63(2):380-389.

Mossey PA, Little J, Munger RG, Dixon MJ, Shaw WC. 2009. Cleft lip and palate. Lancet. 374(9703):1773-1785.

Peters H, Neubuser A, Kratochwil K, Balling R. 1998. Pax9-deficient mice lack pharyngeal pouch derivatives and teeth and exhibit craniofacial and limb abnormalities. Genes Dev. 12(17):2735-2747.

Szabo-Rogers HL, Smithers LE, Yakob W, Liu KJ. 2010. New directions in craniofacial morphogenesis. Dev Biol. 341(1):84-94.

Twigg SR, Wilkie AO. 2015. New insights into craniofacial malformations. Human molecular genetics. 24(R1):R50-59.

Voutilainen M, Lindfors PH, Trela E, Lonnblad D, Shirokova V, Elo T, Rysti E, Schmidt-Ullrich R, Schneider P, Mikkola ML. 2015. Ectodysplasin/nf-kappab promotes mammary cell fate via wnt/beta-catenin pathway. PLoS Genet. 11(11):e1005676.

Weatherley-White RC, Sakura CY, Jr., Brenner LD, Stewart JM, Ott JE. 1972. Submucous cleft palate. Its incidence, natural history, and indications for treatment. Plast Reconstr Surg. 49(3):297-304.

Zhang Y, Tomann P, Andl T, Gallant NM, Huelsken J, Jerchow B, Birchmeier W, Paus R, Piccolo S, Mikkola ML et al. 2009. Reciprocal requirements for eda/edar/nf-kappab and wnt/beta-catenin signaling pathways in hair follicle induction. Dev Cell. 17(1):49-61.

Zhang Y, Zhao X, Hu Y, St Amand T, Zhang M, Ramamurthy R, Qiu M, Chen Y. 1999. Msx1 is required for the induction of patched by sonic hedgehog in the mammalian tooth germ. Developmental dynamics : an official publication of the American Association of Anatomists. 215(1):45-53.

Zhou J, Gao Y, Lan Y, Jia S, Jiang R. 2013. Pax9 regulates a molecular network involving bmp4, fgf10, shh signaling and the osr2 transcription factor to control palate morphogenesis. Development. 140(23):4709-4718.

Zhou J, Gao Y, Zhang Z, Zhang Y, Maltby KM, Liu Z, Lan Y, Jiang R. 2011. Osr2 acts downstream of pax9 and interacts with both msx1 and pax9 to pattern the tooth developmental field. Dev Biol. 353(2):344-353.

Figure Legends

Figure 1. Expression profiles of Eda/Edar signaling pathway-related genes in E13.5 palatal shelves.

(**A**) Table of RNAseq data showing raw counts of Eda/Edar signaling pathway-related genes selected from RNAseq data. Compared with Pax9+/+ samples, Edar expression was significantly downregulated in Pax9−/−samples. FC, fold change; *P < 0.01.

(**B**) The mRNA levels were confirmed by real-time RT-PCR (n = 5). Error bars indicate SEM, *P < 0.01.

Figure 2. NF-**κ**B activity and Eda/Edar signaling during palate formation.

(A–D) LacZ staining of NF-**κ**B reporter (rep) embryos from E12.5 to E15.

Signals appeared at the center of the lingual edge of the palate at E12.5 (A). At E13, the signals elongated along the palatal edge (B). At E14, the signals were on the rugae and throughout the lingual edge of the palate (C). At E15, the palatal shelves fused and the signals remained on the rugae (D).

(E–L) Comparison of the expression of Edar and Eda mRNAs in the palatal shelves of Pax9−/−and Pax9+/− embryos. Whole-mount in situ hybridization of Edar at E13.5 (E, F) and E14.5 (I, J). Pax9−/−embryos (E, I) showed strong expression along the lingual region of the developing palate shelves (red arrow heads) and incisor tooth germs (red *), whereas Pax9−/− embryos (F, J) showed decreased expression levels in both palate shelves and incisors.

Whole-mount in-situ hybridization of Eda at E13.5 (G, H) showed similar expression level in Pax9+/− (G) and Pax9−/−embryos (H). At E14.5 (K, L), Eda had a specific expression in the lingual region of the posterior palate in Pax9+/− (K, black arrows), and this pattern was diffused in Pax9−/− (L). * indicates incisor tooth germ; red arrowheads indicate lingual region of palate shelves; black arrows indicate posterior palate. Scale bar, 100 μm.

Figure 3. Treatment with mAbEDAR monoclonal antibody corrected cleft palate defects in Pax9−/− embryos.

(**A**) Schematic diagram showing the delivery timeline of mAbEDAR monoclonal antibodies. a, single injection at E10.5; b, 2 injections at E10.5 and E12.5.

(**B**) Table summarizes secondary palate closure with mAbEDAR monoclonal antibody treatment in Pax9−/− embryos. *, number of Pax9−/− embryos with incomplete fusion between the primary and secondary palates (see Appendix Fig. 2).

Figure 4. Secondary palate fusion in Pax9−/− embryos after mAbEDAR monoclonal antibody treatments.

Representative photographs of palate formation at E18.5 in control treated Pax9+/+ (A, D), Pax9−/− (B, E) and mAbEDAR monoclonal antibody treated Pax9−/− (C, F) with the injection timeline at E10.5. The whole-mount oral view of palatal shelf showed cleft palates in control Pax9−/− embryos (n = 10) (B) and palate closure with disordered rugae in mAbEDAR monoclonal antibody treated Pax9-/- embryos (n = 19) (C). Hematoxylin and eosin-stained (D-F) coronal sections showed fusion of the palatal shelves in control Pax9+/+ (D) and mAbEDAR monoclonal antibody treated Pax9−/− (F) embryos. * indicates cleft palate; black arrows indicate secondary palate fusion after treatment; T, tongue; arrowheads indicate intact palate shelve. Scale bars, 100 μm.

Figure 5. Restored osteogenesis in the palate of E18.5 Pax9−/− mice treated with mAbEDAR monoclonal antibody.

Masson's trichrome staining (A–F) of coronal sections showed that the palatal shelves were fused in control Pax9+/+ (A, D) and mAbEDAR monoclonal antibod-treated Pax9−/− (C, F), whereas complete cleft was found in control Pax9−/− (B, E). Connective tissue is stained blue, nuclei are dark red/purple, and the cytoplasm is red/pink. (G–L) Comparison of Col1a1 expression in the palatal bone formation of Pax9+/− and Pax9−/− embryos with mAbEDAR monoclonal antibody treatment v. control. Position-matched coronal sections of E18.5 embryos through the anterior and posterior palates are used. mRNA signals are shown in blue. The red arrow indicates osteogenic centers of the developing palatal processes of the maxilla; the red arrowheads indicate prospective palatal processes of the palatine bone. A high-powered view of palatal fusion zones is shown in black rectangle boxes.

A

Gene	*Pax9*$^{+/+}$	*Pax9*$^{-/-}$	FC	pvalue
Edar	179.67	106.60	0.59*	0.0016
Edaradd	771.71	616.13	0.80	0.0171
Eda	1446.81	1543.39	1.07	0.0335
Eda2r	129.34	131.37	1.02	0.9980
Tab2	10029.67	10580.25	1.05	0.2540
Chuk (Ikka)	2345.27	2412.69	1.03	0.7399
Ikbkb (Ikkβ)	2382.61	2466.28	1.04	0.9974
Traf6	1942.60	1893.92	0.97	0.9084
Nr2c2 (TAK1)	4898.71	4957.44	1.01	0.7475
Ikbkg (Nemo)	1817.35	1834.87	1.01	0.7858

B

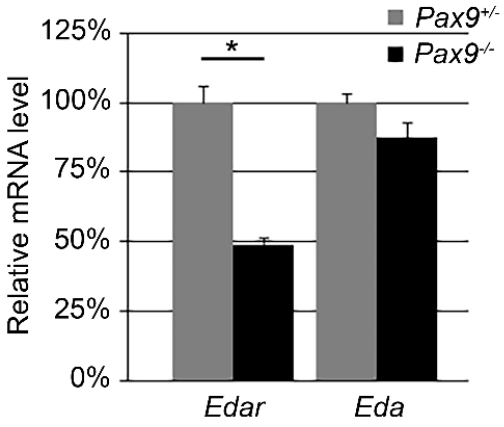

Figure 1.

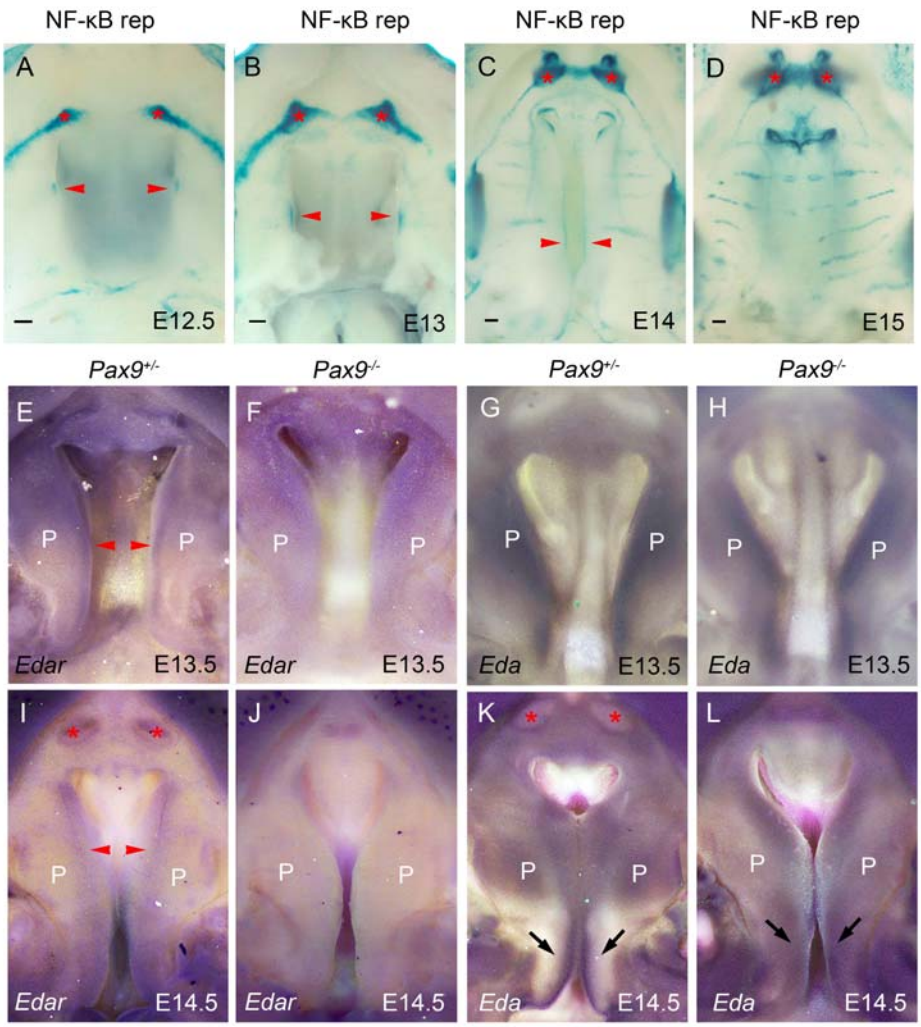
NF-κB rep
NF-κB rep
NF-κB rep
NF-κB rep
A
B
C
D
E12.5
E13
E14
E15
Pax9+/-
Pax9-/-
Pax9+/-
Pax9-/-
E
F
G
H
P
Edar E13.5
Edar E13.5
Eda E13.5
Eda E13.5
I
J
K
L
Edar E14.5
Edar E14.5
Eda E14.5
Eda E14.5

Figure 2.

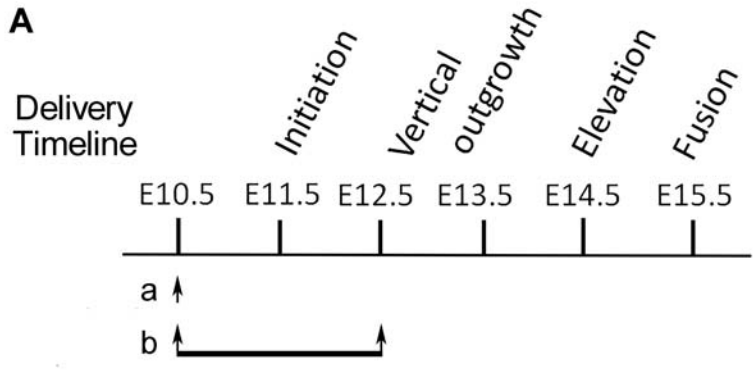

B

Timeline	Dosage (mg/Kg)	*Pax9*$^{-/-}$ No.	Closure	Cleft Palate
E10.5	16	14	10 (4*)	4
E10.5/12.5	16	10	9 (3*)	1

Figure 3.

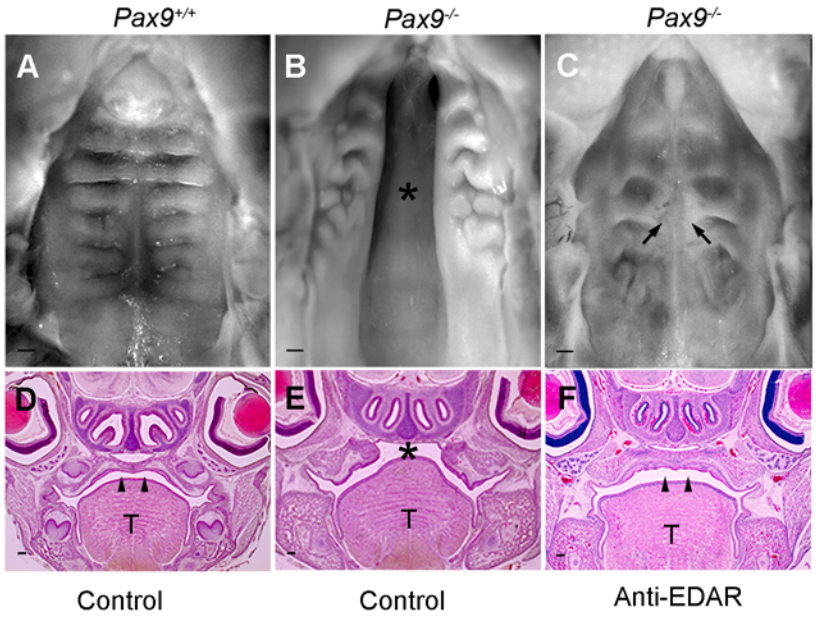

Figure 4.

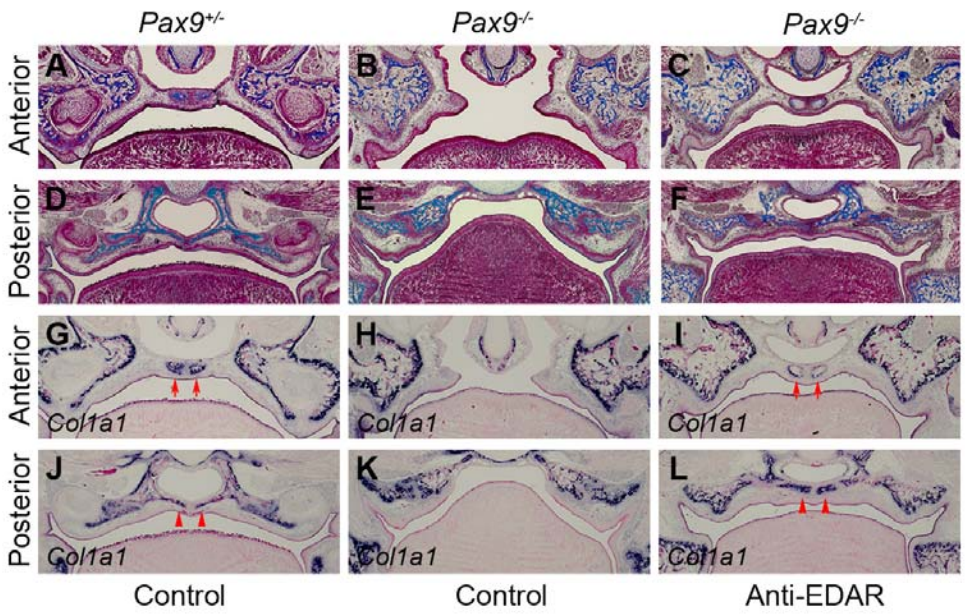

Figure 5.

Supplementary Table S1. Primers for Real-time RT-PCR:

Name	Sequence (5'-3')
Edar-QF	ACAGTCAAGAGCGAGTTCCC
Edar-QR	AGTACACCTGGTACCCGAAT
Eda-QF	AGGTGGAGTGCTCAATGACTG
Eda-QR	CGATTTTCTGCCTGGCCTTG
GAPDH-QF	TGGAGCCAAAAGGGTCA
GAPDH-QR	CTTCTGGGTGGCAGTGA